DOI: 10.1002/ejic.201001024

Compact Metal–Organic Frameworks for Anti-Corrosion Applications: New Binary Linear Saturated Carboxylates of Zinc

Adel Mesbah,[a] Sophie Jacques,[a] Emmanuel Rocca,*[a] Michel François,[a] and Jean Steinmetz[a]

Keywords: Metal–organic frameworks / Zinc / Carboxylate ligands / X-ray diffraction / Surface chemistry

Zinc-based metal–organic frameworks (MOFs), binary zinc carboxylates $ZnC_nC_{n'}$ with C_n and $C_{n'} = CH_3(CH_2)_{n-2}COO^-$, have been synthesised and characterised for anti-corrosion applications. The crystallographic structures of $ZnC_{10}C_{14}$ and $ZnC_{10}C_{16}$ were determied from synchrotron powder diffraction data and refined by the Rietveld method. Protective coatings on electrogalvanised steel composed of $ZnC_{12}C_{16}$ have been developed by formulating a particular "carboxylating" bath. The $ZnC_{12}C_{16}$ coating exhibits better anti-corrosion behaviour than the pure $Zn(C_{16})_2$ and $Zn(C_{12})_2$ coatings, according to electrochemical and non-electrochemical measurements. The crystallographic results and corrosion measurements demonstrate the great flexibility of the zinc carboxylate lamellar structures in modifying the insolubility and hydrophobicity of the protective coatings. In addition, the conditions for the $ZnC_{12}C_{16}$ coating process fulfil the specifications for the surface treatment of zinc. Finally, these new compounds, which can be easily synthesised in water, provide a new and environmentally friendly anti-corrosion treatment for metals.

Introduction

For several years, much work has been focused on the implementation of a "green" treatment of metals. For this purpose, the ability of saturated straight-chain aliphatic monocarboxylates to inhibit the corrosion of Fe, Cu, Mg, Pb and Zn in aerated solutions has been investigated.[1] The carboxylate anions, $CH_3(CH_2)_{n-2}COO^-$ (noted C_n^-), act as a converting agent at the metal surface in the presence of oxidants H_2O_2, BO_3^- or O_2. Thus, once a critical concentration of cations (Fe^{3+}, Cu^{2+} or Zn^{2+}) is reached at the metal/electrolyte interface a metallic soap film grows.

In contrast to research on the use of porous metal–organic frameworks (MOFs) in catalysis or absorption applications,[2] the use of these compounds in anti-corrosion treatment requires the construction of close-packed MOFs on the metallic surface. The objective is to synthesise very insoluble and hydrophobic MOFs.

In the case of zinc, the growth of protective MOFs on the surface depends on the pH. Thin layers are formed in neutral or slightly basic media and can be used for the temporary protection of metals during storage for example, or in the cooling water of heat exchanger equipment. As proved by several analytical techniques, the protective film is formed of a layered zinc hydroxycarboxylate, $Zn_5(C_7)_2(OH)_8$, in the case of a heptanoate compound.[3] On the other hand, both thick and well-crystallised films formed only of $Zn(C_n)_2$-based compounds with $n = 7$ and 10 can be quickly elaborated in an acidic medium. This acid treatment, called "carboxylating", appeared to be an effective and a suitable replacement for phosphating or phosphating/chromating processes.[4]

Recently, the crystallographic structures of zinc monocarboxylates $Zn(C_n)_2$ with short- and mid-length carbon chains were solved on the basis of single-crystal[5] and synchrotron powder diffraction data.[6] All the structures are characterised by a lamellar stacking of polymeric sheets $[Zn(C_n)_2]_x$ perpendicular to the longest axis (c axis). The sheets are linked by van der Waals interactions and made up of a plane of zinc atoms parallel to (00l). The ZnO_4 tetrahedrons are linked by bidentate and bridging carboxylates, whereas the distance between the Zn atom planes (also named interlayer distance d_0) varies regularly and depends on the number of carbon atoms (Figure 1). Thus, the stability is closely dependent upon the aliphatic chain length, and this property induces a decrease in the solubility of the zinc carboxylate $[Zn(C_n)_2]$ as the carbon chain length increases.

From a chemical engineering viewpoint, saturated fatty acids HC_n having a high number of carbon atoms are handicapped by their weak solubility in aqueous baths and their high melting points. For example, stearic acid HC_{18} has a melting point of 68 °C. These compounds need to operate at high temperature, at around 55 °C, in a hydro-

[a] Institut Jean Lamour – UMR CNRS 7198, Université Henri Poincaré, Nancy Université,
54506 Vandoeuvre les Nancy, France
Fax: +33-3-83466811
E-mail: emmanuel.rocca@lcsm.uhp-nancy.fr

Supporting information for this article is available on the WWW under http://dx.doi.org/10.1002/ejic.201001024.

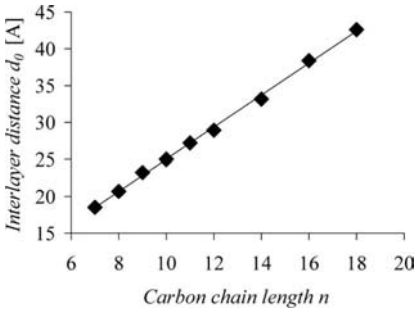

Figure 1. Interlayer distance d_0 of $Zn(C_n)_2$ vs. the carbon chain length (from ref.[5,6]).

organic solution containing 60 vol.-% of organic solvent. These conditions are not readily compatible with industrial applications of the surface treatment of zinc.

Thus, we have prepared new baths formed of mixtures of two single carboxylic acids, HC_n and $HC_{n'}$, with a composition corresponding to the eutectic point of the binary diagram[7] in order to use liquid acid baths at a lower carboxylating treatment temperature, about 45 °C. Moreover, the existence of intermediate phases in the binary diagrams of even saturated fatty acids with a formula of $H_2C_nC_{n'}$ led us to expect mixed zinc salts. Indeed, 10 binary zinc carboxylates $Zn(C_n)_{2x}(C_{n'})_{2-2x}$ (with $18 \geq n$ and $n' \geq 10$) were synthesised and then characterised by crystallography.

Finally, the coating of a binary zinc carboxylate was performed on a zinc substrate by using the "carboxylating" process. Its corrosion behaviour was characterised by electrochemical and non-electrochemical measurements and compared with single zinc carboxylate coatings.

Results

Structural Resolution on Powder

Syntheses engaging two single acids were performed in aqueous solvent according to reaction (1).

$$Zn(NO_3)_2 + 2x\ NaC_n + 2(1-x)\ NaC_{n'} \rightarrow Zn(C_n)_{2x}(C_{n'})_{2-2x} + 2\ Na^+ + 2\ NO_3^- \quad (1)$$

$x = 0.1, 0.3, 0.5, 0.7, 0.9$

For $x < 0.5$, the XRD pattern of the single zinc carboxylate with the longest carbon chain is systematically observed, whereas for $x > 0.5$ two families of diffraction peaks are present, one belonging to the XRD pattern of the shorter carboxylate and the other, attributed to a new compound, a binary zinc carboxylate.

For $x = 0.5$, only this new zinc soap was detected, so its formula could be $ZnC_nC_{n'}$. Two examples of X-ray diffraction patterns of pure binary zinc carboxylates are shown in Figure 2 and compared with those of their equivalent single carboxylates.

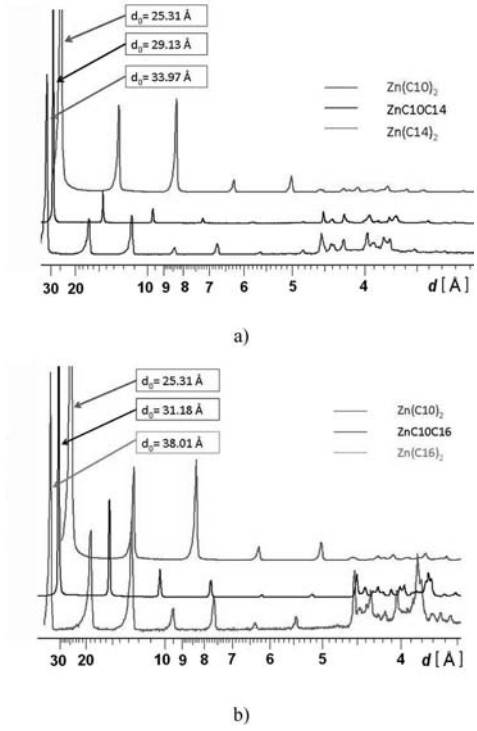

Figure 2. X-ray diffraction patterns of $ZnC_{10}C_{14}$ and $ZnC_{10}C_{16}$ superimposed on those of the single carboxylates of zinc, $Zn(C_{10})_2$, $Zn(C_{14})_2$ and $Zn(C_{16})_2$.

In all cases, for $x = 0.5$, the measured interlayer distances obtained by small-angle X-ray scattering (SAXS) are very close to those calculated from the arithmetic average of the single zinc carboxylates (d_0; Table 1).

It can be expected that each binary soap layer is formed of two half layers of the single zinc carboxylates $Zn(C_n)_2$ and $Zn(C_{n'})_2$. Thus, as shown in Figure 3, these 10 binary zinc carboxylates should also adopt a lamellar crystallographic organisation, C_n–Zn–$C_{n'}$, with $x = 0.5$ with the general formula $Zn(C_n)_{2x}(C_{n'})_{2-2x}$.

By using the powder XRD data obtained at the European Synchrotron Radiation Facility (ESRF, Grenoble, France), the crystallographic structures of the two binary compounds $ZnC_{10}C_{14}$ and $ZnC_{10}C_{16}$ were completely resolved. The first standard peak search with X-cell[8] permitted the indexation of the two powder patterns in the triclinic $P1$ space group, with the following lattice parameters. $ZnC_{10}C_{14}$: $a = 4.76$, $b = 4.78$, $c = 29.11$ Å, $\alpha = 94.95$, $\beta = 95.51$, $\gamma = 70.69°$ with FOM (figure of merit) = 1074. $ZnC_{10}C_{16}$: $a = 4.76$, $b = 4.78$, $c = 31.08$ Å, $\alpha = 94.56$, $\beta = 94.56$, $\gamma = 70.94°$ with FOM = 1211.

Profile matching procedures on the two patterns were performed successfully and led to good agreement factors with polarisation resistance $R_p = 5.6\%$, $R_{wp} = 7.1$, $\chi^2 = 3.0$ for $ZnC_{10}C_{14}$ and $R_p = 4.6\%$, $R_{wp} = 6.5$, $\chi^2 = 1.97$ for $ZnC_{10}C_{16}$.

The atoms were localised in direct space by ab initio methods using the FOX program.[9] The two monocarboxylate chains were introduced as rigid bodies by using the Z-matrix without H atoms, and the zinc atom was located in

Table 1. Comparison of the interlayer distances d_0 of single zinc carboxylates $Zn(C_n)_2$ and binary zinc carboxylates $ZnC_nC_{n'}$ calculated and measured by SAXS.

n	n'	$d_0[Zn(C_n)_2]$[a] [Å]	$d_0[Zn(C_{n'})_2]$[a] [Å]	Calculated $d_0[ZnC_nC_{n'}]$ [Å]	Measured $d_0[ZnC_nC_{n'}]$ [Å]
10	12	25	29.4	27.20	27.50
10	14		33.9	29.45	29.62
10	16		38.1	31.55	31.53
10	18		42.4	33.70	33.91
12	14	29.4	33.9	31.65	31.78
12	16		38.1	33.75	33.76
12	18		42.4	35.90	36.04
14	16	33.9	38.1	36.00	36.10
14	18		42.4	38.15	38.27
16	18	38.1	42.4	40.25	40.61

[a] From ref.[5,6]

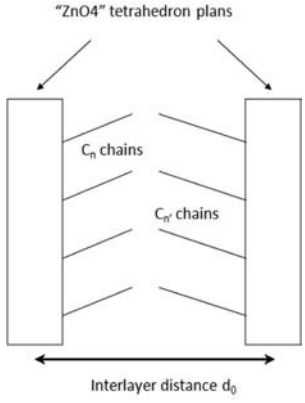

Figure 3. Hypothetical model of a layered mixed carboxylate $ZnC_nC_{n'}$.

the centre of an oxygen tetrahedron. The excess oxygen atoms were corrected by the dynamic occupancy option implemented in the FOX program. Then the model proposed was refined by the Rietveld method using the FULLPROF software.[10] During the refinement, soft constraints were applied on the interatomic distances: d(C–C) = 1.54(1) Å, d(C–O) = 1.25(1) Å and angles C–C–C 109(1)°, O–C–O 120(1)°. The Rietveld refinement of the two compounds led to satisfactory agreement factors (R_{Bragg} = 0.11 for each phase). Data collection and refinement parameters for the two structures are reported in Table 2.

The observed, calculated and difference patterns of $ZnC_{10}C_{16}$ are compared in Figure 4, and fractional coordinates of non-hydrogen atoms are reported in the Supporting Information.

Table 2. Rietveld refinement parameters for $ZnC_{10}C_{14}$ and $ZnC_{10}C_{16}$.

	$ZnC_{10}C_{14}$	$ZnC_{10}C_{16}$
Empirical formula	$Zn(C_{10}H_{19}O_2)(C_{14}H_{23}O_2)$	$Zn(C_{10}H_{19}O_2)(C_{16}H_{31}O_2)$
M [g mol^{-1}]	459.3	491.3
System	triclinic	triclinic
Space group	$P1$	$P1$
a [Å]	4.7802(1)	4.7657(1)
b [Å]	4.7797(1)	4.7833(1)
c [Å]	29.1087(12)	31.0850(4)
α [°]	94.978(3)	93.281(2)
β [°]	95.445(3)	94.569(2)
γ [°]	70.907(3)	70.940(2)
Volume [Å^3]	624.57(3)	667.26(2)
D_x [g cm^{-3}]/Z	1.22/1	1.20/1
Wavelength [Å]	0.851243(1)	0.851243(1)
Absorption coefficient (μr)	0.88	0.83
Angle range [°]	0.711–25.99	0.33–25.99
No. of points observed	8430	8555
N_{ref}	203	227
R_p	0.099	0.080
R_{wp}	0.154	0.109
χ^2	13.6	6.22
R_{Bragg}	0.112	0.114
R_F	0.123	0.10
No. of constraints	32	41
No. of profile parameters	16	8
No. of parameters depending on the intensity	88	94

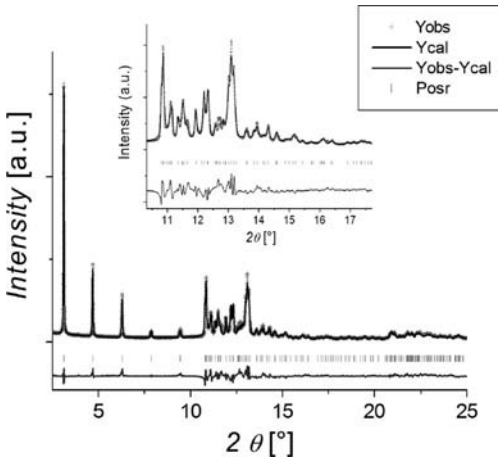

Figure 4. Rietveld refinement of $ZnC_{10}C_{16}$.

The two structures are characterised by a stacking of layers perpendicular to the *c* axis. The general projections of the $ZnC_{10}C_{14}$ and $ZnC_{10}C_{16}$ structures along the *a* axis show that each layer is made up of a plane of ZnO_4 tetrahedrons with carbon chains C_n (C_{10}) and $C_{n'}$ (C_{14} or C_{16}) on both sides, as displayed in the Figure 5.

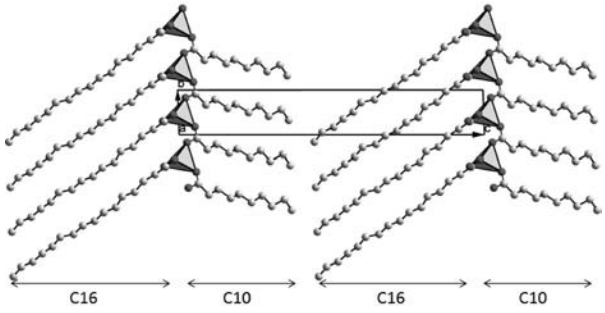

Figure 5. Projection of the structures of $ZnC_nC_{n'}$ along the *a* axis, with $ZnC_{10}C_{16}$ given as an example.

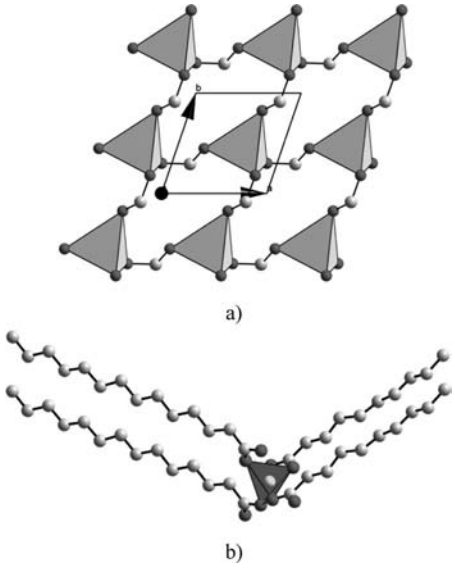

Figure 6. (a) Projection along the *c* axis and (b) basic block of the $ZnC_nC_{n'}$ structure, with $ZnC_{10}C_{14}$ given as an example.

All the tetrahedrons have the same orientation, as in the structures of the single $Zn(C_n)_2$ with *n* even and ≥10 (Figure 6a). The ZnO_4 tetrahedrons are linked by bidentate and bridging carboxylates with chains of the same length always parallel to each other. Finally, the layer organisation of these new crystallographic structures can be described by the basic block represented in the Figure 6b.

The interatomic distances Zn–O vary from 1.980 to 2.008 Å in $ZnC_{10}C_{14}$ and from 1.953 to 2.006 Å in $ZnC_{10}C_{16}$. These distances are in agreement with the anionic radii of the atoms reported in the Shannon tables.[11] The C–C and C–O distances are close to 1.54 and 1.27 Å in the two phases. Selected interatomic distance and angle values are reported in the Supporting Information.

Coating Synthesis and Characterisation

The carboxylating process was carried out in water/3-methoxy-3-methyl-1-butanol (MMB) containing the oxidising agent H_2O_2 and the carboxylic acids. The coatings carried out with the two pure carboxylic acids HC_{12} and HC_{16} were compared with the coating performed with a mixture of HC_{12}/HC_{16} with a composition of that of the eutectic point in the binary diagram.

To use a pure carboxylic acid with a long carbon chain such as HC_{16}, it was necessary to increase the operating temperature to 55 °C and the organic solvent content to solubilise sufficiently the carboxylic acid in the bath. In contrast, the use of the HC_{12}/HC_{16} eutectic mixture, which is liquid at room temperature, allowed us to operate at 45 °C with a 50:50 vol.-% water/MMB. The operative conditions are summarised in Table 3.

Table 3. Carboxylating process conditions for different bath compositions.

Carboxylating bath[a]	*T* [°C]	$[HC_n]$[b] [g L^{-1}]	Water/MMB [vol.-%]	XRD analysis
HC_{12}	45	60	50:50	ZnC_{12}
HC_{16}	55	77	40:60	ZnC_{16}
HC_{12}/HC_{16}	45	45:19	50:50	$ZnC_{12}C_{16}$

[a] All carboxylating baths contain 5 g of H_2O_2 per L^{-1}. [b] All HC_n concentrations correspond to 0.3 mol L^{-1}.

Figure 7 shows that the coating weight increases sharply during the first seconds of the carboxylating process and then reaches a plateau. A very high coating weight was attained with the acid with the longest carbon chain length, HC_{16}.

Taking the coating kinetics into account, electrogalvanised steel sheets were treated for less than 15 s with a view to an industrial application and in order to have a coating weight of around 1.5 g m^{-2}, similar to the coating weights produced in phosphating treatments. As expected, the coatings formed in the HC_{12} and HC_{16} baths contain single zinc carboxylates, $Zn(C_{12})_2$ or $Zn(C_{16})_2$, according to the XRD analysis reported in Table 3. In the case of the

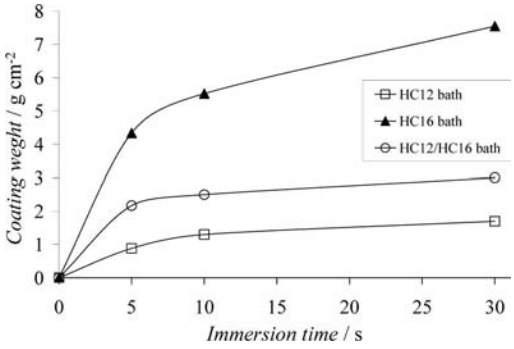

Figure 7. Coating weight vs. immersion time in three carboxylating baths.

binary HC_{12}/HC_{16} bath, the coating is formed only of the binary zinc carboxylate, $ZnC_{12}C_{16}$.

Concerning the morphology, the soap crystals are relatively small in all three cases, around 5–10 μm, as shown in Figure 8a,c,e. Nevertheless, the $Zn(C_{16})_2$ coating on zinc, as revealed by the SEM images in backscattered electron (BSE) mode, exhibits many uncovered zones (white zones) in comparison with the $Zn(C_{12})_2$ and $ZnC_{12}C_{16}$ coatings, which have very good coverage (black zones).

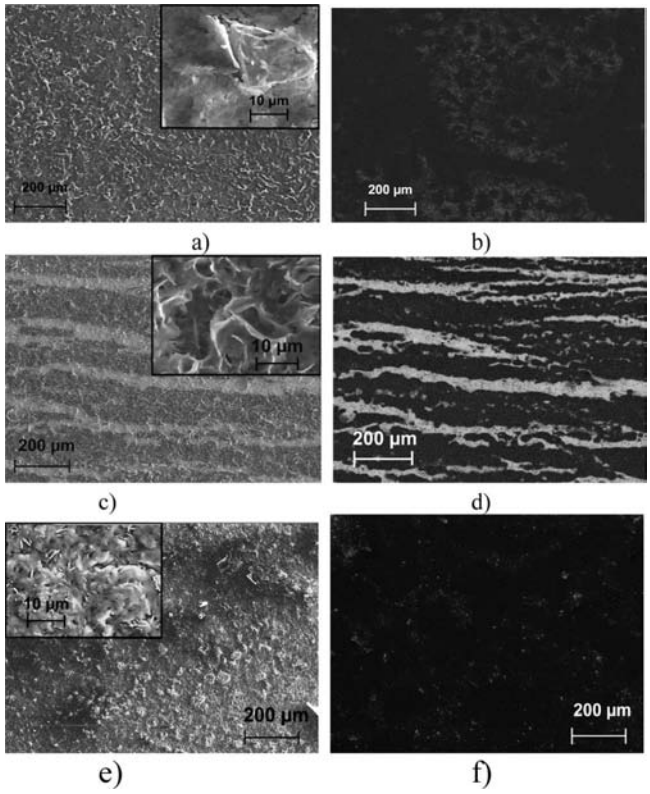

Figure 8. SEM images of electrogalvanised steel after (a),(b) HC_{12}, (c),(d) HC_{16} and (e),(f) HC_{12}/HC_{16} carboxylation processing (the processing conditions are given in Table 2). The photos in (b), (d) and (f) are in phase contrast (BSE mode).

Electrochemical measurements of corrosion resistance were carried out in a reference corrosive water (ASTM D 1384-87 standard, noted ASTM). The results are compared with those obtained from the experiment performed on untreated electrogalvanised steel.

Whatever the bath, the corrosion potentials of the coated samples are larger than those obtained with the untreated sample, as clearly shown in Figure 9a. These high values of corrosion potential reveal that all the zinc carboxylate coatings inhibit the anodic reaction of zinc dissolution. The binary coating is clearly the most efficient.

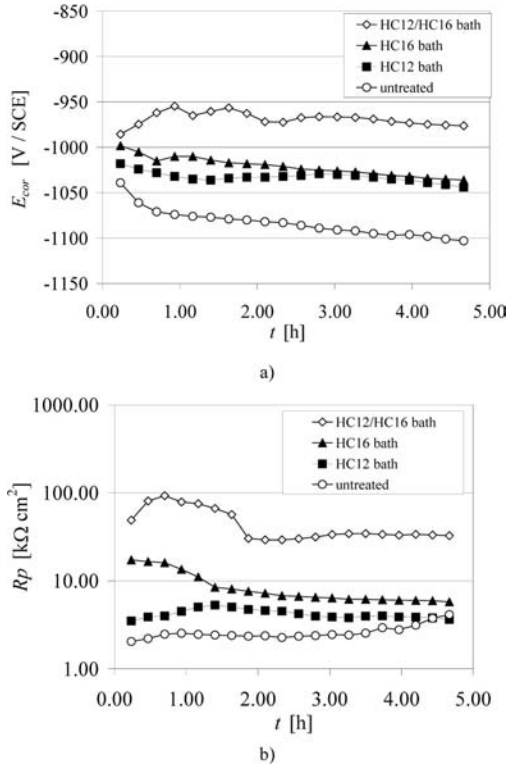

Figure 9. Evolution of (a) corrosion potential and (b) polarisation resistance of untreated and treated electrogalvanised steel as a function of immersion time (coating weight: 1.5 $g\,m^{-2}$).

According to the R_p measurements (Figure 9b), all the deposits show a higher polarisation resistance than the untreated sample and form an efficient passive layer on electrogalvanised steel. Nevertheless, after 2–3 h of immersion in corrosive water, the R_p values of samples protected by pure HC_{12} or HC_{16} decrease to that of the untreated electrogalvanised steel. In contrast, the $ZnC_{12}C_{16}$ coating displays the best corrosion behaviour under these conditions with a relatively constant and larger value of R_p as well as a higher corrosion potential.

To complete the study of the corrosion behaviour of these coatings, climatic chamber tests involving successive wet/dry cycles were performed over approximately 2 months.

According to Figure 10, the percentage of zinc surface covered with white rust versus the number of climatic cycles reveals that after five cycles the untreated electrogalvanised steel is entirely covered with white rust, formed of $Zn(OH)_2$ and $Zn_5(CO_3)_2(OH)_6$, as proved by XRD. The

$Zn(C_{16})_2$ coating is more resistant, but the best results were observed with the $Zn(C_{12})_2$ and $ZnC_{12}C_{16}$ coatings, which were not very corroded after 20 wet/dry cycles. Note the binary zinc carboxylate coating exhibits good anti-corrosion behaviour even after 65 wet/dry cycles.

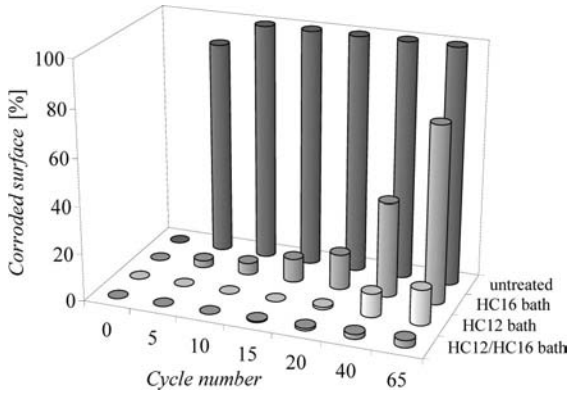

Figure 10. Corrosion of untreated and treated electrogalvanised steels as a function of wet/dry cycles.

Note that the climatic chamber tests, more realistic for testing the cosmetic corrosion of zinc, are consistent with the electrochemical results obtained under immersion conditions. Thus, this kind of coating could provide zinc with long-term corrosion resistance against the development of white rust compounds.

Discussion and Conclusions

One of the strategies for the design of new compounds to protect the metallic substrate against corrosion is to build an insoluble and hydrophobic layer acting as a barrier against corrosion reactions. For that, compact metal–organic frameworks can be good candidates if the conditions of chemical synthesis are compatible with industrial conditions. This kind of coating should be able to replace some phosphating treatments carried out on electrogalvanised steels during the automotive processes.

Previous work has proved that the protection produced by the carboxylating process increases with the length of the straight alkyl chains. This parameter is crucial, because it strongly influences the solubility of the zinc carboxylate soap. Indeed, the cohesion of the structure is assured by the electrostatic interactions in the ZnO_4 planes and also by the van der Waals forces between the aliphatic chains on both sides of these planes.

According to the results, the $Zn(C_{12})_2$ layer exhibits interesting anti-corrosion properties, but they are not sufficient to protect electrogalvanised steel for 2 months in a climatic chamber. In contrast, the $Zn(C_{16})_2$ layer exhibits bad corrosion behaviour despite the fact that this compound has a longer carbon chain length. In fact, the surface coverage of $Zn(C_{16})_2$ is much lower than that of $Zn(C_{12})_2$ even though the $Zn(C_{16})_2$ layer has a high coating weight.

A possible explanation lies in the differences in the processing conditions. In fact, the use of a pure long-chain carboxylic acid demands a higher bath temperature and a modified solvent composition. This change of parameters increases the solubility of $Zn(C_n)_2$ in the bath, modifying the conditions of crystallisation on the metallic surface and thus the coverage of the coatings.

Consequently, it is necessary to use "soft" processing conditions to synthesise the MOFs with long carbon chains on zinc metal to increase the insolubility and hydrophobicity of the protective layer.

This objective was achieved by using in the carboxylating bath a mixture of two fatty acids, HC_n and $HC_{n'}$, in a ratio corresponding to the eutectic point of the binary system. The surface treatment did not lead to the deposition of two separate zinc carboxylates, $Zn(C_n)_2$ and $Zn(C_{n'})_2$, nor only the more insoluble, but to the growth of an original soap that has a structure derived from a combination of the two single carboxylates.

These new MOFs are characterised by an alternation of short and long chains in the C_n–Zn–$C_{n'}$ sequence, as proved by the structure determinations of $ZnC_{10}C_{14}$ and $ZnC_{10}C_{16}$. Eight other binary Zn carboxylates have been synthesised with the same crystallographic organisation. All these compounds are probably isostructural or have very similar structures. The stability of the $C_{n'}$–Zn–C_n layer is also ensured by both the ionic interactions between the carboxylate group $–COO^-$ and the zinc cations Zn^{2+} in the plane of the ZnO_4 tetrahedrons and the van der Waals interactions between the CH_2 groups of two adjacent carbon chains in different layers. The 3D cohesion between the layers is mainly a result of the van der Waals interactions between the terminal CH_3 groups of each monocarboxylic acid. The surface coverage of the $ZnC_{12}C_{16}$ coating is similar to that of the $Zn(C_{12})_2$ coating, but its solubility is lower {pK[$Zn(C_{12})_2$] = 14.4; pK($ZnC_{12}C_{16}$) = 15.8}, which explains why it has the best anti-corrosion properties. The coating formed from only $Zn(C_{16})_2$ is less soluble {pK[$Zn(C_{16})_2$] = 15.8} and more hydrophobic, but its poor homogeneity on the surface explains its poor anti-corrosion behaviour.

Now more complex carboxylating mixtures have to be tested, with three or more fatty acids. Perhaps they would lead to further improvements in the protection of metals and allow new phases, ternary, quaternary, to be identified that will enrich the zinc carboxylate family. Clearly, this approach will lead to bath compositions closely related to the fatty acid mixtures produced by European flowering plants. The crystallographic results have demonstrated the great flexibility of the lamellar structures of zinc carboxylates. It has been proved that carboxylate chains can easily be exchanged in original binary zinc carboxylate structures. Now it is tempting to expect such exchange ability with cations, namely cations with higher charges.

Finally, the use of these new flexible compounds, which can be easily synthesised in aqueous solvent, provides an interesting approach to new and environmentally friendly anti-corrosion treatment of metals.

Experimental Section

Synthesis of Single and Binary Zinc Carboxylates as Powders: Crystallised powders of zinc carboxylates have been synthesised in aqueous solution by the addition of sodium carboxylates to zinc nitrate solution. During the addition, the solution was maintained at 65 °C and pH = 5. Then the white precipitate was filtered, washed with distilled water and finally dried in a desiccator. The solubility of the different compounds was determined by Zn^{2+} analysis with ICP-AES.

Powder X-ray Diffraction Study: The X-ray diffraction patterns of the mixtures were compared with those of the single zinc carboxylates, $Zn(C_n)_2$ and $Zn(C_{n'})_2$. The distances between the layers of ZnO_4 tetrahedrons were evaluated by SAXS (small-angle X-ray scattering) using an INEL XRG 3000 diffractometer equipped with a Cu anti-cathode. For structural resolution, X-ray powder diffraction data were collected at the European Synchrotron Radiation Facility (ESRF) by using the synchrotron radiation of the very high resolution powder diffractometer installed on the beam line ID31.[12] A primary double-crystal monochromator Si(111) was used for selecting the wavelength. Detection was ensured by a nine-consecutive-crystals Ge(111) analyser. Each sample as a fine white powder was introduced into a Lindeman tube (Φ = 1 mm). The samples were spun on the axis of the diffractometer. Each capillary was translated along the axis to give a fresh region of sample every 15 min to avoid radiation damage. Data were recorded by using a wavelength of 0.851243(4) Å at 100 K with an interval of 0.003° and a total counting time of 2 h. CCDC-791660 ($ZnC_{10}C_{14}$) and -791661 ($ZnC_{10}C_{16}$) contain the supplementary crystallographic data for this paper. These data can be obtained free of charge from The Cambridge Crystallographic Data Centre via www.ccdc.cam.ac.uk/data_request/cif.

Coating Process and Characterisation: Coatings were performed on square and double-faced zinc electrogalvanised steel sheets [provided by Arcelor Mittal (France)] by using a home-made pilot.[1] The different steps of the coating process are as follows. The steel sheets were degreased in an alkaline bath containing Gardoclean S 5225 and Gardobond H 7352 (Chemetal) at 55 °C for 360 s. They were then rinsed with deionised water at room temperature for 60 s before carboxylating at 45 and 55 °C. After coating, the film morphology was examined by using a Philips XL30 scanning electron microscope equipped with a Kevex Sigma EDS in the secondary electron and backscattered electron modes with an acceleration voltage of 10 keV. On the zinc surface, the different phases [zinc, zinc(II) carboxylate] were identified by energy-dispersive X-ray (EDX) spectroscopy by measuring the C/Zn ratio and by imaging the surface in the backscattered electron (BSE) mode. The surface compounds were analysed by X-ray diffraction with an X'Pert Pro-Philips diffractometer by using Cu-$K_{\alpha 1}$ and Cu-$K_{\alpha 2}$ wavelengths (λ_1 = 1.54051 Å and λ_2 = 1.54433 Å). The coating weight was determined by measuring the weight difference between the "carboxylated" sample and the same sample after coating dissolution under ultrasound in 1,1-dichloroethane.

Electrochemical Measurements and Corrosion Tests: The electrochemical tests were performed under aerated conditions with a three-electrode electrochemical cell connected to an EGG PAR 273A potentiostat driven by a computer. In this configuration, the circular working electrode surface is vertical facing the Pt disk counter-electrode. The reference electrode was a KCl saturated calomel electrode (Hg/Hg_2Cl_2; E = +0.242 V/SHE), and all the working electrode potentials were measured relative to this reference. The corrosive medium used as reference in the electrochemical experiments was the ASTM D 1384-87 solution (noted ASTM) with the following composition: 148 mg L^{-1} Na_2SO_4, 138 mg L^{-1} $NaHCO_3$ and 165 mg L^{-1} NaCl. The polarisation resistances (R_p) were recorded over 5 h with measurements performed every 15 min at a scan rate of 0.166 mV s^{-1} for a range of 20 mV (E_{corr} = ±10 mV). Test cycles in the climatic chamber (KBEA 300, LIEBISCH) were carried out to simulate atmospheric corrosion: 8 h at 100% of humidity using twice-distilled water heated at 40 °C followed by 16 h under ambient conditions.

Supporting Information (see footnote on the first page of this article): Selected interatomic distances and fractional positions of atoms in the structures of $ZnC_{10}C_{14}$ and $ZnC_{10}C_{16}$.

Acknowledgments

The authors would like to thank the ADEME AGRICE for funding this study and Arcelor, Total Lubrifiant for their support.

[1] a) C. Georges, E. Rocca, P. Steinmetz, *Electrochim. Acta* **2008**, *53*, 4839–4845; b) S. Jacques, E. Rocca, M. J. Stebe, J. Steinmetz, *Surface Coatings Technol.* **2008**, *202*, 3878–3885; c) E. Rocca, G. Bertrand, C. Rapin, J. C. Labrune, *J. Electroanal. Chem.* **2001**, *503*, 133–140; d) J. Peultier, E. Rocca, J. Steinmetz, *Corros. Sci.* **2003**, *45*, 1703–1716; e) E. Rocca, J. Steinmetz, *Corros. Sci.* **2001**, *43*, 891–902.
[2] a) M. Edgar, R. Mitchell, A. M. Z. Slawin, P. Lightfoot, P. A. Wright, *Chem. Eur. J.* **2001**, *7*, 5168–5175; b) Q.-R. Fang, G.-S. Zhu, M. Xue, Q.-L. Zhang, J.-Y. Sun, X.-D. Guo, S.-L. Qiu, S.-T. Xu, P. Wang, D.-J. Wang, Y. Wei, *Chem. Eur. J.* **2006**, *12*, 3754–3758; c) M. Eddaoudi, J. Kim, D. Vodak, A. Sudik, J. Wachter, M. O'Keeffe, O. M. Yaghi, *Proc. Natl. Acad. Sci. USA* **2002**, *99*, 4900–4904.
[3] E. Rocca, C. Caillet, A. Mesbah, M. Francois, J. Steinmetz, *Chem. Mater.* **2006**, *18*, 6186–6193.
[4] E. Rocca, C. Rapin, F. Mirambet, *Corros. Sci.* **2004**, *46*, 653–665.
[5] a) J. Peultier, M. François, J. Steinmetz, *Acta Crystallogr., Sect. C: Cryst. Struct. Commun.* **1999**, *55*, 2064–2065; b) F. Lacouture, J. Peultier, M. François, J. Steinmetz, *Acta Crystallogr., Sect. C: Cryst. Struct. Commun.* **2000**, *56*, 556–557; c) A. Mesbah, C. Juers, F. Lacouture, S. Mathieu, E. Rocca, M. François, J. Steinmetz, *Solid State Sci.* **2007**, *9*, 322–328.
[6] A. Mesbah, C. Juers, M. François, E. Rocca, J. Steinmetz, *Z. Kristallog. Suppl.* **2007**, *26*, 593.
[7] a) D. Feldman, M. M. Shapiro, D. Banu, C. J. Fuks, *Sol. Energy Mater.* **1989**, *18*, 201–216; b) M. C. Costa, M. Sardo, M. P. Rolemberg, J. A. P. Coutinho, A. J. A. Meirelles, P. Ribeiro-Claro, M. A. Krähenbüh, *Chem. Phys. Lipids* **2009**, *160*, 85.
[8] M. A. Neumann, *J. Appl. Crystallogr.* **2003**, *36*, 356–365.
[9] a) R. Černý, V. Favre-Nicolin, *Powder Diffr.* **2005**, *20*, 359–365; b) R. Černý, V. Favre-Nicolin, *Z. Kristallogr.* **2007**, *222*, 105–113.
[10] T. Roisnel, J. Rodriguez-Carvajal, *WinPLOTR: A windows tool for powder diffraction pattern analysis*, Materials Science Forum, 7th European Powder Diffraction Conference (EPDIC 7), Barcelona, Spain, **2001**, pp. 118–123.
[11] R. D. Shannon, *Acta Crystallogr., Sect. A* **1976**, *32*, 751–767.
[12] A. N. Fitch, *J. Res. Natl. Inst. Stand. Technol.* **2004**, *109*, 133–142.

Received: September 26, 2010
Published Online: January 21, 2011

